

Quantifying the Errors Introduced by Continuum Scattering Models on the Inferred Structural Properties of Proteins[†]

Rohan S. Adhikari,[‡] Dilipkumar N. Asthagiri,^{*,¶} and Walter G. Chapman^{*,‡}

[‡]*Department of Chemical and Biomolecular Engineering, Rice University, 6100 Main St., Houston, TX 77005, USA*

[¶]*Oak Ridge National Laboratory, One Bethel Valley Road, Oak Ridge, TN 37830-6012*

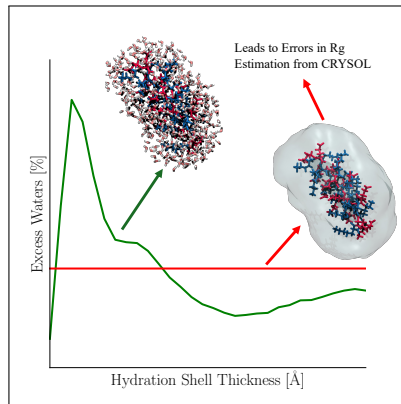
E-mail: asthagiridn@ornl.gov; wgchap@rice.edu

Abstract

Atomistic force fields that are tuned to describe folded proteins predict overly compact structures for intrinsically disordered proteins (IDPs). To correct this, improvements in force fields to better model IDPs are usually paired with scattering models for validation against experiments. For scattering calculations, protein configurations from all-atom simulations are used within the continuum-solvent model CRY SOL for comparison with experiments. To check this approach, we develop an equation to evaluate the radius of gyration (R_g) for any defined inner-hydration shell thickness given all-atom simulation data. R_g based on an explicit description of hydration waters compares well with the reference value of R_g obtained using Guinier analysis of the all-atom scattering model. However, these internally consistent estimates disagree with R_g from CRY SOL for the

same definition of the inner-shell. CRY SOL can over-predict R_g by up to 2.5 Å. We rationalize the reason for this behavior and highlight the consequences for force field design.

TOC Graphic



[†]Notice: This manuscript has been authored by UT-Battelle, LLC, under contract DE-AC05-00OR22725 with the US Department of Energy (DOE). The US government retains and the publisher, by accepting the article for publication, acknowledges that the US government retains a nonexclusive, paid-up, irrevocable, worldwide license to publish or reproduce the published form of this manuscript, or allow others to do so, for US government purposes. DOE will provide public access to these results of federally sponsored research in accordance with the DOE Public Access Plan (<https://www.energy.gov/doe-public-access-plan>)

Intrinsically Disordered Proteins (IDPs) have garnered tremendous scientific interest due to their ability to remain functional despite being disordered.¹⁻⁵ The consensus in the scientific community links their malleable structural properties to a variety of intracellular phenomena such as the formation of membraneless organelles^{6,7} and the regulation of signalling networks.^{8,9} When they misfire due to aggregation or mutation they are known to cause a host of pathologies such as amyloidosis^{10,11} or cardiovascular diseases.^{12,13} Traditional force field based simulation models were tuned to replicate the properties of folded proteins and have been shown to predict overly compact structures for IDPs.¹⁴⁻¹⁸ Numerous modifications to force fields have been proposed to circumvent this issue.¹⁹⁻²³ Such modifications need to be validated against experimental data. Due to the availability of high flux synchrotron sources and data analysis programs, Small Angle X-ray Scattering (SAXS) is one of the most widely used methods in such studies.²⁴⁻²⁶

In SAXS both the solute and the solvent contribute to the scattered intensity. Relative to a neat solvent, the presence of the solute affects scattering by the solvent in two specific ways: (1) by excluding a volume that would otherwise be occupied by the solvent, and (2) by associating with an excess of solvent in the inner-hydration shell.²⁷ In the so-called process of background subtraction^{26,28} the role of the bulk solvent is sought to be removed from the scattering profile of the protein-solvent mixture. The remaining signal is interpreted to infer properties of the protein conformation. It is clear that the specific role of the solute on the solvent needs to be treated as a part of the solute, and to this end, scattering models are necessary to translate the simulated coordinates to experimentally measurable quantities.

CRY SOL was the first model to account for the specific effects of the solute on the solvent. It does so by assuming a continuum bulk density of the solvent in the excluded volume region and a continuum excess density of the solvent in the solvation layer.^{29,30} The program FoXS expedites the scattering computations by strategically placing dummy solvent atoms around the

exposed surface of the solute in solution.^{31,32} The importance of accounting for more density variation in the solvation layer was recognized by Park et. al.³³ who proposed an explicit water scattering model that incorporates the solvation layer in atomic detail. Virtanen et. al. used the detailed hydration layer predicted by the program HyPred³⁴ to calculate the SAXS profiles of proteins.³⁵ Similarly, Poitevin et. al. used the solvent maps generated by AquaSol³⁶ in their program AquaSAXS.³⁷ All of the scattering models discussed so far assume a frozen solute which is enough to accurately describe the scattering in the Guinier regime. For a full SAXS comparison the thermal fluctuations of the solute also need to be included.³⁸ The program WAXSIS,³⁹ incorporating both the thermal fluctuation of the solute and an atomic solvation layer, is currently the gold standard for simulated X-ray scattering.^{40,41}

Simulation studies have largely been indifferent to the improvements in scattering models noted above. CRY SOL is frequently the model of choice when force fields are validated against SAXS data.^{14,15,42} Most notably CRY SOL was used in the development of the CHARMM36m force field for IDP simulations.²¹ CRY SOL’s computational speed and ease of use are two of the major reasons for its continued use despite the availability of more detailed models.^{26,30} Even though the assumption of a uniform excess density in the hydration layer has been called into question by several explicit water simulation studies,^{35,38,43} the consequences of this approximation on the scattering predictions made by CRY SOL have not been adequately understood. We believe it is imperative to define metric(s) that allow for the validation of scattering models by studying their predictions in isolation. We develop such a metric.

All of the scattering models in literature seek to mimic the experimental background subtraction procedure represented in Eq. 1.^{26,44}

$$\Delta I(q) = I_A(q) - I_B(q) \quad (1)$$

Park et. al.³³ came up with an equation that computes the background subtracted intensities

for simulated structures of biomolecules. One of the advantages of their formalism is the ability to incorporate an atomistic hydration layer. The simulated background subtraction procedure is graphically represented in Fig. 1A and 1B. The framework developed in Ref. 33 which we shall henceforth call the explicit water scattering model is shown in Eq. 2.

$$\Delta I(q) = \left\langle \left| \langle A(\mathbf{q}) \rangle - \langle B(\mathbf{q}) \rangle \right|^2 + \left[\langle |A(\mathbf{q})|^2 \rangle - \langle |A(\mathbf{q})|^2 \rangle \right] - \left[\langle |B(\mathbf{q})|^2 \rangle - \langle |B(\mathbf{q})|^2 \rangle \right] \right\rangle_{\Omega} \quad (2)$$

A and B in Eq. 2 correspond to the amplitudes from the protein-water simulation and the bulk water simulation, respectively. An envelope of a defined volume is carved out of the protein-water simulation box (Fig. 1A). A similar envelope of the same volume is carved out of the bulk water simulation box (Fig. 1B). The behavior of waters outside this envelope is assumed to be bulk-like. The volume of the envelope is usually defined based on the distance from solute atoms. Moving a distance 7 Å away from all solute atoms is known to be enough to reach bulk-like behavior of water.^{33,38} In our work the hydration shell is defined to be 3 Å thick from the surface of the solute atoms to maintain consistency with the CRY SOL description.^{26,45} This choice also ensures that the binding energy of the solute with the solvent outside the inner-shell admits a Gaussian description,⁴⁶⁻⁴⁸ signalling non-specific interactions.

The CRY SOL model (Eq. 3)

$$\Delta I(q) = \langle |A_p(\mathbf{q}) - \rho_b A_{ex}(\mathbf{q}) + \delta \rho_h A_h(\mathbf{q})|^2 \rangle_{\Omega} \quad (3)$$

is a simplification of the explicit water scattering model. In a continuum density description, the terms in Eq. 2 which account for density fluctuations vanish,³³ and the amplitude difference between the protein-water system and the bulk water system is defined in terms of an excess density parameter ($\delta \rho_h$) for the hydration shell and a volume parameter (V_{ex}) for the excluded volume.²⁹

The CRY SOL model can be used either by inputting a hydration layer contrast or by varying the parameters in Eq. 3 to get the best fit to the experimental data.³⁰ The CRY SOL model does not require a bulk water simulation to perform the subtraction and is graphically represented in Fig. 1C.

Our internal consistency check to quantify the errors that arise from a continuum hydration description (Eq. 3) is as follows. For a defined inner-hydration shell thickness, Eq. 4 is used to calculate the R_g from the coordinates of the protein-hydration layer complex. (N_A and N_B are the total number of atoms in the protein and the hydration layer and the number of atoms in the same volume of a bulk water simulation respectively. N_F is the total number of simulated frames. See the SI for further details.)

$$R_g^{coor} = \sqrt{\frac{\sum_{N_F} \sum_{N_A} n_A^e |\mathbf{r}_A - \mathbf{r}_{com}|^2 - \sum_{N_F} \sum_{N_B} n_B^e |\mathbf{r}_B - \mathbf{r}_{com}|^2}{\sum_{N_F} \sum_{N_A} n_A^e - \sum_{N_F} \sum_{N_B} n_B^e}}, \quad (4)$$

where,

$$\mathbf{r}_{com} = \frac{\sum_{N_F} \sum_{N_A} n_A^e \mathbf{r}_A - \sum_{N_F} \sum_{N_B} n_B^e \mathbf{r}_B}{\sum_{N_F} \sum_{N_A} n_A^e - \sum_{N_F} \sum_{N_B} n_B^e} \quad (5)$$

The R_g calculated using Eq. 4 is compared to the R_g predicted from Guinier analysis^{49,50} of the scattering curve. (Fig. S1 provides a schematic of the consistency check.) In our work the hydration layer definition in Eq. 4 is consistent with CRY SOL and hence the R_g from the two methods can be directly compared. Inconsistency between these measures serves to signal potential failures of either the definition of the inner-shell thickness or the continuum approximation or both.

When MD simulations are paired with CRY SOL and validated against experimental data the errors from the scattering model alone cannot be isolated. By assuming a hydration shell that is 3 Å thick and by supplying the contrast calculated from explicit water simulations (see the SI for details) as an input to CRY SOL,

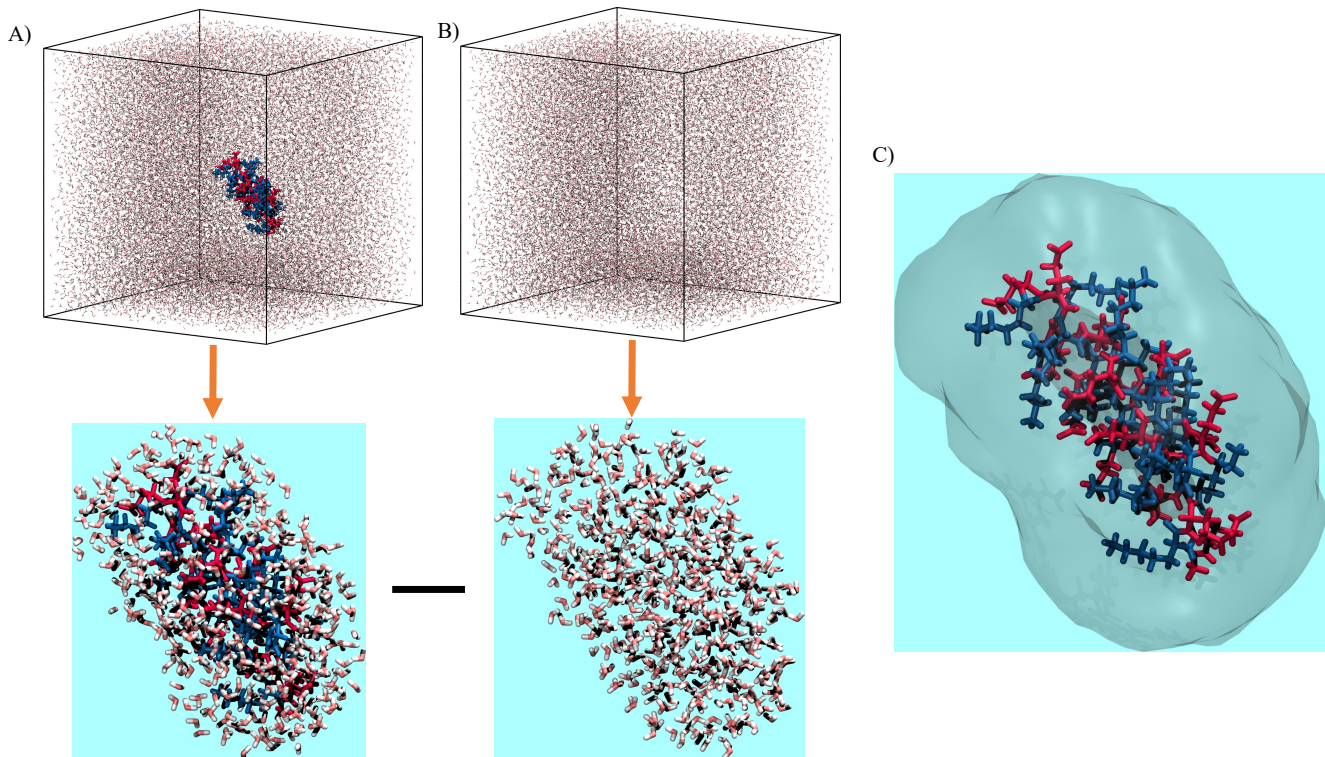


Figure 1: Schematic representation of scattering models. Panels (A) and (B) together constitute the explicit water scattering model. The intensity from a bulk water simulation (B) is subtracted from the intensity of a protein-water simulation (A). The continuum scattering model is represented in (C). The blue background in (A), (B) and (C) represents the bulk-like solvent which is treated as a continuum.

we ensure that there is a direct correspondence between the explicit water scattering model (Eq. 2), the R_g calculation from coordinates (Eq. 4) and the CRY SOL model (Eq. 3). In this way we have devised a consistency check that can isolate the errors due to a continuum description of the hydration layer.

We chose 20 protein structures from the Protein Data Bank (PDB). The same 20 proteins were used to predict the hydration layer around proteins in the HyPred³⁵ program. The proteins were simulated in explicit water using NAMD.⁵¹ The solute was frozen during the simulation and was modeled using the CHARMM36m (C36m)²¹ force field. Modified TIP3P waters (m-TIP3P)⁵² were used in all simulations. All of the explicit water scattering calculations and the R_g calculations were performed using in-house PYTHON scripts. The MDTraj⁵³ library was used to load the NAMD trajectory files. All of the CRY SOL calcu-

lations were performed using CRY SOL 3.0.³⁰ Fig. 2 shows the errors from CRY SOL and the explicit water scattering model.

ΔR_g in Fig. 2 represents the difference between the R_g prediction made by the scattering model and the R_g calculated from the coordinates (Eq. 4). ΔR_g for CRY SOL is always positive and is as high as 2.5 Å. The errors from CRY SOL remain significant irrespective of the contrast in the hydration layer (Fig. 2A) or the size of the protein (Fig. 2B). ΔR_g for the explicit water scattering model is very close to 0 Å. Hence it represents the information in the system accurately.

CRY SOL can also be used to fit to the experimental data by varying the parameters in Eq. 3. The problem of overfitting in CRY SOL has previously been studied for protein-detergent complexes.⁵⁴ However quantifying the errors in R_g from this approach is not easy, because the experimental data does not correspond to the

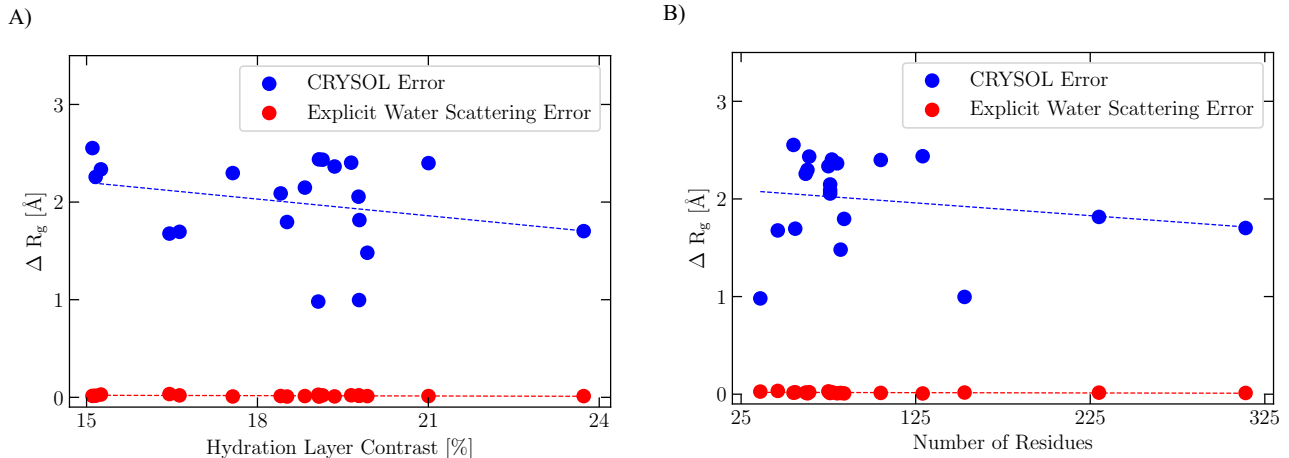


Figure 2: Errors from the explicit water scattering model are shown in red. Errors from CRY SOL are shown in blue. The errors from the scattering models are plotted against the hydration layer contrast in (A) and the size of the protein in (B). Best fit lines are a guide to the eye.

solute alone but is a property of the protein-hydration layer complex. A variety of solute structures with different R_g can be combined with appropriate excess density parameters in CRY SOL to obtain good fits against the experimental data. The fitting procedure used in CRY SOL is represented by Eq. 6

$$\chi^2 = \frac{1}{N} \sum_{i=1}^N \left[\frac{f I_{calc}(q_i) - I_{ref}(q_i)}{\sigma_{ref}(q_i)} \right]^2, \quad (6)$$

where $I_{calc}(q_i)$ are the intensities predicted by CRY SOL, $I_{ref}(q_i)$ are the intensities predicted by the explicit water scattering model, and $\sigma_{ref}(q_i)$ are the error bars from the explicit water scattering model. A factor of f (Eq. 6) is used in the fitting procedure to scale the predictions from the scattering model to the same units as the reference. This has no consequence to the shape of the scattering curve and hence the properties of interest.

Fitting to the experimental data does not provide any information about the difference in the solute R_g between experiments and CRY SOL. To circumvent this issue, we fit CRY SOL to the explicit water scattering data. This way the R_g of the underlying solute is known exactly in addition to the scattering data of the protein-water complex. The explicit water scattering data for reference structures of four dif-

ferent proteins are obtained by freezing the solute. Eight protein structures for each of the four proteins with R_g ranging from 2.5 Å lower than the reference and 1 Å higher than the reference are selected. The protein structure and the explicit water scattering data are input into CRY SOL. This workflow is shown in schematic Fig. S2.

In Fig. 3, χ^2 values for all eight structures are plotted against the ΔR_g of the solute. ΔR_g is the difference between the R_g of the structure and the R_g of the reference. A χ^2 value less than 0.5 is considered an excellent fit (probability of the fit: 1.000), while a χ^2 value less than 1.0 is considered a good fit (probability of the fit: 0.460). Using the χ^2 measure, structures 2.5 Å **more compact** than the reference are frequently shown to be excellent fits by CRY SOL. Our results call into question this practice of using χ^2 as a measure of the accuracy of scattering models. CRY SOL does a better job of discriminating between structures that are more expanded than the reference. This is because of the innate proclivity of CRY SOL to overpredict the R_g of the system. Both by contrast matching and by fitting CRY SOL to the reference we find that it has a tendency to over-estimate the effect of the excess waters on the R_g of the system. We will explain the rationale for this divergence below.

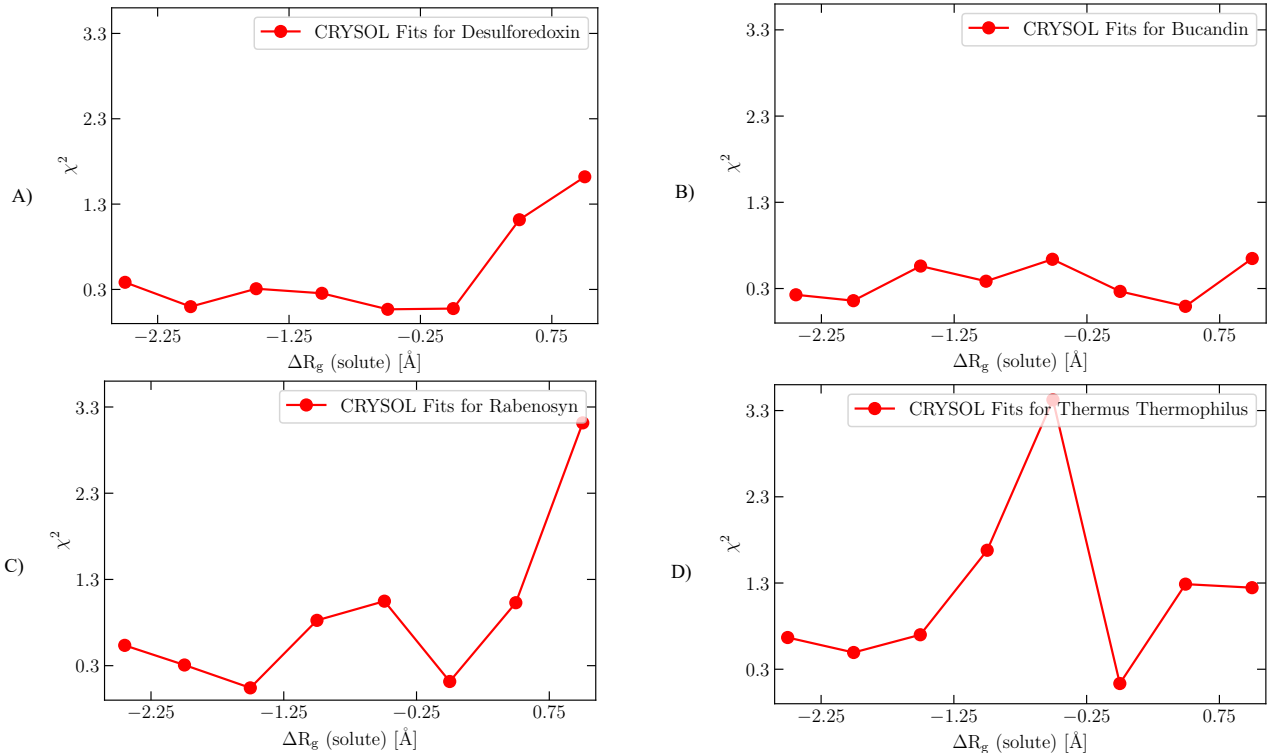


Figure 3: χ^2 values for 8 structures of the protein plotted against the difference in R_g between the structure in question and the reference (ΔR_g). The four proteins used in the study are (A) Desulforedoxin (PDB code: 1DXG), (B) Bucandin (PDB code: 1F94), (C) Rabenosyn (PDB code: 1YZM), and (D) Thermus Thermophilus (PDB code: 2ZQE).

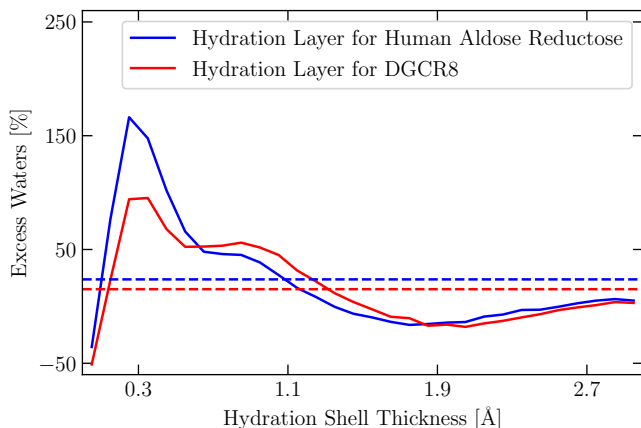
To understand the overprediction from CRY SOL, let us look closely at the distribution of waters in the hydration layer. The distribution of waters for two proteins from explicit water simulations are shown in Figure 4A. The distribution shows a characteristic sharp peak close to the surface of the protein (within 1 Å from the surface) and then a dip in the density from about 1-3 Å from the protein surface. Figure 4A also shows the distribution of waters if it were a continuum (dotted lines).

In the continuum density framework, waters will have to be moved from the surface of the protein to the outer edges of the hydration shell to maintain a constant contrast. This movement of waters away from the protein surface (shown in Fig. 4B) increases the R_g of the protein-water complex and significantly distorts the information in the system. Henriques et. al.⁴⁰ reported that good fits were obtained by CRY SOL only when the contrast was set to unphysically low values (around 3 %). The con-

trast for proteins is expected to be in the range of 5-20 %.²⁶ The findings in Ref. 40 further enunciate our point about the over-prediction in R_g from CRY SOL. The alternate approach to using a low contrast within the continuum description would be to vary the hydration shell thickness. However, the full consequences of these approaches to the underlying physics of scattering need to be understood first.

Thermal fluctuations of the protein are not considered in this work for which there are two main reasons. Firstly, the continuum scattering equation used in CRY SOL is not easily extendable to account for thermal fluctuations. Some groups have attempted to use CRY SOL to understand the physics of fluctuating proteins but the ensemble averaging techniques used in these studies are questionable and need further investigation.^{42,55} Second and most importantly, mere fluctuations alone do not cause a deviation in R_g which is the primary quantity of interest here. The arguments and data for this claim

A)



B)

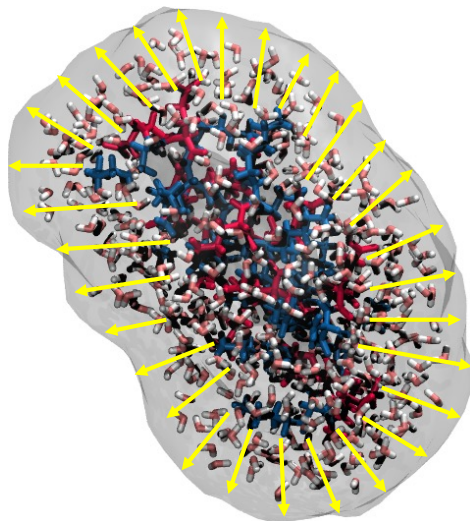


Figure 4: The distribution of waters from an explicit water simulation (solid lines) are shown for two proteins as a function of the hydration shell thickness in (A). The two proteins studied are Human Aldose Reductose (PDB code: 1US0) and DGCR8 (PDB code: 3LE4). The continuum distribution for both proteins are shown in dotted lines in (A). The movement of the waters away from the protein surface which leads to the over-prediction by CRY SOL is graphically represented in (B).

are provided in the Sec. S6 (SI).

In addition to the drawbacks of the continuum density description (addressed here) there are also questions about the definition of the hydration shell in CRY SOL. CRY SOL uses an angular envelope function to geometrically define the shape of the protein and its surrounding hydration shell.^{26,29} This method is known to be accurate for relatively simple shapes (globular proteins) but its applicability to the conformations of IDPs in solution is questionable and needs to be investigated further.²⁶ The division of the envelope into an excluded volume and the hydration shell is a requirement of the continuum solvent approach. Since the explicit water scattering model uses an atomistic description of the solvent such a division is not necessary. This further highlights the need for using the explicit water scattering model in the validation of IDP-specific force field improvements.

On a larger note, the equation developed in this work to calculate the R_g directly from the coordinates of an explicit water simulation (Eq. 4) provides a credible consistency check to validate the Guinier analysis based R_g pre-

diction from any scattering model. R_g is often the quantity used in simulation studies to estimate the ability of force field improvements to capture the properties of extended IDP ensembles.^{21,23,42} When understood in this context the importance of the methodology developed in this work becomes clearer. Zheng et. al.⁵⁰ have suggested that the q range (usually a q_{\max} of $1.3/R_g$) used in the Guinier analysis of experimental scattering profiles is too broad and can lead to errors in R_g estimation by up to 10% for IDPs. A q_{\max} of $1.3/R_g$ is used in experiments due to the difficulty in obtaining high quality background subtracted scattering data at lower q values. However, this problem does not arise for theoretical scattering models. The q_{\max} value in theoretical models can be set as close to zero as required to conform accurately to the approximations in Guinier analysis.

The explicit water scattering model displays a high degree of consistency to the data obtained from simulations. The R_g of the solute alone is also known in addition to the scattering curve which is not possible in experiments. These ad-

vantages were used here to show that it is possible to obtain good χ^2 fits from CRY SOL even for solute structures that are significantly more collapsed than the reference. The methodology used in this work for CRY SOL can be applied to quantify the over-fitting from any general scattering model with free parameters.

Several methods of generating simulated structures of IDPs have been proposed recently and are in need of validation. In our work so far we have explained the limitations of popular implicit solvent models in predicting accurate conformations for polyampholytes.^{48,56} In the near future we also plan to evaluate the performance of IDP-specific improvements to explicit water force fields. Scattering models when used correctly can act as powerful discriminatory tools that aid in the further development of such models.

In conclusion, we have developed a methodology here that allows for an effective validation of scattering models. By isolating the predictions from the scattering model, the methodology negates any possible bias in the analysis that could arise from external errors (such as errors from force fields). Our results suggest that the commonly used χ^2 metric is not a reliable indicator of the accuracy of scattering models. By matching the hydration layer contrast from explicit water simulations, we found CRY SOL to distort the R_g of the system by about 2 Å. By fitting CRY SOL to the explicit water scattering data, its tendency to over-predict the R_g of the system was re-established from a different perspective. This is particularly significant since the difference in the R_g predictions from contemporary force fields is on the order of 2-3 Å. The errors from the explicit water scattering model were almost 2 orders of magnitude lower than those from CRY SOL. The average absolute error from the explicit water scattering model was about 0.02 Å (1.99 Å from CRY SOL), which is of no consequence to the studies of interest. Hence we strongly recommend the use of the explicit water scattering model in foundational studies such as force field validation.

Supporting Information

The Supporting Information includes (1) a schematic of the consistency check and χ^2 over-fitting, (2) additional simulation details, (3) details on the contrast and excluded volume calculation, (4) details on scattering computation and R_g estimation, (5) scattering code validation, and (6) a note on the effect of the thermal fluctuations on the R_g of the system.

Acknowledgements

We thank Dr. Amanda B. Marciel and Winnie H. Shi for engaging discussions about SAXS. RSA would like to thank Dr. Jochen S. Hub for his insights on the theory of scattering models. DA thanks Fred Poitevin for encouraging comments. We thank Dr. Arjun Valiya Parambathu for his help in creating images. We thank the Robert A. Welch foundation for financial support (Grant No. C-1241). We gratefully acknowledge the computational time on Anvil GPUs at the Rosen Center for Advanced Computing (RCAC), Purdue University, and on Stampede2 at the Texas Advanced Computing Center (TACC), University of Texas at Austin. Computational time on these clusters was obtained under a National Science Foundation (NSF) Advanced Cyberinfrastructure Coordination Ecosystem (ACCESS) project (Allocation no. CHM-230024). Research at Oak Ridge National Laboratory is supported under contract DE-AC05-00OR22725 from the U.S. Department of Energy to UT-Battelle, LLC.

References

- (1) Wright, P. E.; Dyson, H. J. Intrinsically Unstructured Proteins: Re-Assessing the Protein Structure-Function Paradigm. *J. Mol. Biol.* **1999**, *293*, 321–331.
- (2) Uversky, V. N. Natively Unfolded Proteins: A Point where Biology waits for Physics. *Prot. Sci.* **2002**, *11*, 739–756.
- (3) Heery, D. M.; Kalkhoven, E.; Hoare, S.; Parker, M. G. A Signature Motif in Tran-

- scriptional Co-Activators Mediates Binding to Nuclear Receptors. *Nature* **1997**, *387*, 733–736.
- (4) Janknecht, R.; Hunter, T. Transcriptional Control: Versatile Molecular Glue. *Curr. Biol.* **1996**, *6*, 951–954.
- (5) Romero, P.; Obradovic, Z.; Kissinger, C. R.; Villafranca, J. E.; Garner, E.; Guilliot, S.; Dunker, A. K. Thousands of Proteins likely to have Long Disordered Regions. *Pac. Symp. Biocomput.* **1998**, *3*, 437–447.
- (6) Wei, M.-T.; Elbaum-Garfinkle, S.; Holehouse, A. S.; Chen, C. C.-H.; Feric, M.; Arnold, C. B.; Priestley, R. D.; Pappu, R. V.; Brangwynne, C. P. Phase Behaviour of Disordered Proteins Underlying Low Density and High Permeability of Liquid Organelles. *Nat. Chem.* **2017**, *9*, 1118–1125.
- (7) Shin, Y.; Brangwynne, C. P. Liquid Phase Condensation in Cell Physiology and Disease. *Science* **2017**, *357*, eaaf4382.
- (8) Bondos, S. E.; Dunker, A. K.; Uversky, V. N. Intrinsically Disordered Proteins play Diverse Roles in Cell Signaling. *Cell Commun. Signal* **2022**, *20*, 20.
- (9) Babu, M. M.; van der Lee, R.; de Groot, N. S.; Gsponer, J. Intrinsically Disordered Proteins: Regulation and Disease. *Curr. Opin. Struct. Biol.* **2011**, *21*, 432–440.
- (10) Uversky, V. N. Amyloidogenesis of Natively Unfolded Proteins. *Curr. Alzheimer Res.* **2008**, *5*, 260–287.
- (11) Mukhopadhyay, S. The Dynamism of Intrinsically Disordered Proteins: Binding-Induced Folding, Amyloid Formation, and Phase Separation. *J. Phys. Chem. B* **2020**, *124*, 11541–11560.
- (12) Cheng, Y.; LeGall, T.; Oldfield, C. J.; Dunker, A. K.; Uversky, V. N. Abundance of Intrinsic Disorder in Protein Associated with Cardiovascular Disease. *Biochem.* **2006**, *45*, 10448–10460.
- (13) Monti, S. M.; De Simone, G.; Langella, E. The Amazing World of IDPs in Human Diseases II. *Biomol.* **2022**, *12*, 369.
- (14) Rieloff, E.; Skepö, M. Molecular Dynamics Simulations of Phosphorylated Intrinsically Disordered Proteins: A Force Field Comparison. *Int. J. Mol. Sci.* **2021**, *22*, 10174.
- (15) Henriques, J.; Cragnell, C.; Skepo, M. Molecular Dynamics Simulations of Intrinsically Disordered Proteins: Force Field Evaluation and Comparison with Experiment. *J. Chem. Theory Comput.* **2015**, *11*, 3420–3431.
- (16) Best, R. B. Computational and Theoretical Advances in Studies of Intrinsically Disordered Proteins. *Curr. Opin. Struct. Biol.* **2017**, *42*, 147–154.
- (17) Huang, J.; MacKerell Jr, A. D. Force Field Development and Simulations of Intrinsically Disordered Proteins. *Curr. Opin. Struct. Biol.* **2018**, *48*, 40–48.
- (18) Nerenberg, P. S.; Head-Gordon, T. New Developments in Force Fields for Biomolecular Simulations. *Curr. Opin. Struct. Biol.* **2018**, *49*, 129–138.
- (19) Wang, W.; Ye, W.; Jiang, C.; Luo, R.; Chen, H.-F. New Force Field on Modeling Intrinsically Disordered Proteins. *Chem. Biol. Drug Des.* **2014**, *84*, 253–269.
- (20) Liu, H.; Song, D.; Zhang, Y.; Yang, S.; Luo, R.; Chen, H.-F. Extensive Tests and Evaluation of the CHARMM36IDPSFF Force Field for Intrinsically Disordered Proteins and Folded Proteins. *Phys. Chem. Chem. Phys.* **2019**, *21*, 21918–21931.
- (21) Huang, J.; Rauscher, S.; Nawrocki, G.; Ran, T.; Feig, M.; De Groot, B. L.; Grubmüller, H.; MacKerell Jr, A. D. CHARMM36m: An Improved Force Field

- for Folded and Intrinsically Disordered Proteins. *Nat. Methods* **2017**, *14*, 71–73.
- (22) Piana, S.; Donchev, A. G.; Robustelli, P.; Shaw, D. E. Water Dispersion Interactions Strongly Influence Simulated Structural Properties of Disordered Protein States. *J. Phys. Chem. B* **2015**, *119*, 5113–5123.
- (23) Shabane, P. S.; Izadi, S.; Onufriev, A. V. General Purpose Water Model can Improve Atomistic Simulations of Intrinsically Disordered Proteins. *J. Chem. Theory Comput.* **2019**, *15*, 2620–2634.
- (24) Lipfert, J.; Doniach, S. Small-Angle X-Ray Scattering from RNA, Proteins, and Protein Complexes. *Annu. Rev. Biophys. Biomol. Struct.* **2007**, *36*, 307–327.
- (25) Bernado, P.; Svergun, D. I. Structural Analysis of Intrinsically Disordered Proteins by Small-Angle X-Ray Scattering. *Mol. Biosyst.* **2012**, *8*, 151–167.
- (26) Svergun, D. I.; Koch, M. H.; Timmins, P. A.; May, R. P. *Small Angle X-Ray and Neutron Scattering from Solutions of Biological Macromolecules*; OUP Oxford, 2013; Vol. 19.
- (27) Serdyuk, I. N.; Zaccai, N. R.; Zaccai, J. *Methods in Molecular Biophysics: Structure, Dynamics, Function*; Cambridge University Press, 2007.
- (28) Bernadó, P.; Mylonas, E.; Petoukhov, M. V.; Blackledge, M.; Svergun, D. I. Structural Characterization of Flexible Proteins using Small-Angle X-Ray Scattering. *J. Amer. Chem. Soc.* **2007**, *129*, 5656–5664.
- (29) Svergun, D.; Barberato, C.; Koch, M. H. CRYSOLO–A Program to Evaluate X-Ray Solution Scattering of Biological Macromolecules from Atomic Coordinates. *J. Appl. Crystallogr.* **1995**, *28*, 768–773.
- (30) Manalastas-Cantos, K.; Konarev, P. V.; Hajizadeh, N. R.; Kikhney, A. G.; Petoukhov, M. V.; Molodenskiy, D. S.; Panjkovich, A.; Mertens, H. D.; Gruzinov, A.; Borges, C. et al. ATSAS 3.0: Expanded Functionality and new Tools for Small-Angle Scattering Data Analysis. *J. Appl. Crystallogr.* **2021**, *54*, 343–355.
- (31) Schneidman-Duhovny, D.; Hammel, M.; Tainer, J. A.; Sali, A. Accurate SAXS Profile Computation and its Assessment by Contrast Variation Experiments. *Biophys. J.* **2013**, *105*, 962–974.
- (32) Schneidman-Duhovny, D.; Hammel, M.; Tainer, J. A.; Sali, A. FoXS, FoXSDock and MultiFoXS: Single-State and Multi-State Structural Modeling of Proteins and their Complexes based on SAXS Profiles. *Nucleic Acids Res.* **2016**, *44*, W424–W429.
- (33) Park, S.; Bardhan, J. P.; Roux, B.; Makowski, L. Simulated X-Ray Scattering of Protein Solutions using Explicit-Solvent Models. *J. Chem. Phys.* **2009**, *130*.
- (34) Virtanen, J. J.; Makowski, L.; Sosnick, T. R.; Freed, K. F. Modeling the Hydration Layer around Proteins: HyPred. *Biophys. J.* **2010**, *99*, 1611–1619.
- (35) Virtanen, J. J.; Makowski, L.; Sosnick, T. R.; Freed, K. F. Modeling the Hydration Layer around Proteins: Applications to Small- and Wide-Angle X-Ray Scattering. *Biophys. J.* **2011**, *101*, 2061–2069.
- (36) Koehl, P.; Delarue, M. AQUASOL: An Efficient Solver for the Dipolar Poisson–Boltzmann–Langevin Equation. *J. Chem. Phys.* **2010**, *132*.
- (37) Poitevin, F.; Orland, H.; Doniach, S.; Koehl, P.; Delarue, M. AquaSAXS: A Web Server for Computation and Fitting of SAXS Profiles with Non-Uniformly Hydrated Atomic Models. *Nucleic Acids Res.* **2011**, *39*, W184–W189.
- (38) Chen, P.-c.; Hub, J. S. Validating Solution Ensembles from Molecular Dynamics Sim-

- ulation by Wide-Angle X-Ray Scattering Data. *Biophys. J.* **2014**, *107*, 435–447.
- (39) Knight, C. J.; Hub, J. S. WAXSiS: A Web Server for the Calculation of SAXS/WAXS Curves based on Explicit-Solvent Molecular Dynamics. *Nucleic Acids Res.* **2015**, *43*, W225–W230.
- (40) Henriques, J.; Arleth, L.; Lindorff-Larsen, K.; Skepö, M. On the Calculation of SAXS Profiles of Folded and Intrinsically Disordered Proteins from Computer Simulations. *J. Mol. Biol.* **2018**, *430*, 2521–2539.
- (41) Hub, J. S. Interpreting Solution X-Ray Scattering Data using Molecular Simulations. *Curr. Opin. Struct. Biol.* **2018**, *49*, 18–26.
- (42) Rauscher, S.; Gapsys, V.; Gajda, M. J.; Zweckstetter, M.; De Groot, B. L.; Grubmüller, H. Structural Ensembles of Intrinsically Disordered Proteins depend Strongly on Force Field: A Comparison to Experiment. *J. Chem. Theory Comput.* **2015**, *11*, 5513–5524.
- (43) Linse, J.-B.; Hub, J. S. Scrutinizing the Protein Hydration Shell from Molecular Dynamics Simulations against Consensus Small-Angle Scattering Data. *Commun. Chem.* **2023**, *6*, 272.
- (44) Grishaev, A.; Guo, L.; Irving, T.; Bax, A. Improved Fitting of Solution X-Ray Scattering Data to Macromolecular Structures and Structural Ensembles by Explicit Water Modeling. *J. Amer. Chem. Soc.* **2010**, *132*, 15484–15486.
- (45) Krywka, C.; Sternemann, C.; Paulus, M.; Javid, N.; Winter, R.; Al-Sawalmih, A.; Yi, S.; Raabe, D.; Tolan, M. The Small-Angle and Wide-Angle X-Ray Scattering Set-Up at Beamline BL9 of DELTA. *J. Synchrotron Radiat.* **2007**, *14*, 244–251.
- (46) Tomar, D. S.; Weber, W.; Pettitt, M. B.; Asthagiri, D. Importance of Hydrophilic Hydration and Intramolecular Interactions in the Thermodynamics of Helix-Coil Transition and Helix-Helix Assembly in a Deca-Alanine Peptide. *J. Phys. Chem. B* **2016**, *120*, 69–76.
- (47) Asthagiri, D. N.; Paulaitis, M. E.; Pratt, L. R. Thermodynamics of Hydration from the Perspective of the Molecular Quasichemical Theory of Solutions. *J. Phys. Chem. B* **2021**, *125*, 8294–8304.
- (48) Adhikari, R. S.; Parambathu, A. V.; Chapman, W. G.; Asthagiri, D. N. Hydration Free Energies of Polypeptides from Popular Implicit Solvent Models Versus All-Atom Simulation Results based on Molecular Quasichemical Theory. *J. Phys. Chem. B* **2022**, *126*, 9607–9616.
- (49) Cantor, C. R.; Schimmel, P. R. *Biophysical Chemistry: Part II: Techniques for the Study of Biological Structure and Function*; Macmillan, 1980.
- (50) Zheng, W.; Best, R. B. An Extended Guinier Analysis for Intrinsically Disordered Proteins. *J. Mol. Biol.* **2018**, *430*, 2540–2553.
- (51) Phillips, J. C.; Hardy, D. J.; Maia, J. D.; Stone, J. E.; Ribeiro, J. V.; Bernardi, R. C.; Buch, R.; Fiorin, G.; Hénin, J.; Jiang, W. et al. Scalable Molecular Dynamics on CPU and GPU Architectures with NAMD. *J. Chem. Phys.* **2020**, *153*.
- (52) Neria, E.; Fischer, S.; Karplus, M. Simulation of Activation Free Energies in Molecular Systems. *J. Chem. Phys.* **1996**, *105*, 1902–1921.
- (53) McGibbon, R. T.; Beauchamp, K. A.; Harrigan, M. P.; Klein, C.; Swails, J. M.; Hernández, C. X.; Schwantes, C. R.; Wang, L.-P.; Lane, T. J.; Pande, V. S. MDTraj: A Modern Open Library for the Analysis of Molecular Dynamics Trajectories. *Biophys. J.* **2015**, *109*, 1528–1532.

- (54) Chen, P.-c.; Hub, J. S. Structural Properties of Protein–Detergent Complexes from SAXS and MD Simulations. *J. Phys. Chem. Lett.* **2015**, *6*, 5116–5121.
- (55) Yang, S.; Park, S.; Makowski, L.; Roux, B. A Rapid Coarse Residue-Based Computational Method for X-Ray Solution Scattering Characterization of Protein Folds and Multiple Conformational States of Large Protein Complexes. *Biophys. J.* **2009**, *96*, 4449–4463.
- (56) Shi, W. H.; Adhikari, R. S.; Asthagiri, D. N.; Marciel, A. B. Influence of Charge Block Length on Conformation and Solution Behavior of Polyampholytes. *ACS Macro Lett.* **2023**, *12*, 195–200.

Supporting Information:

Quantifying the Errors Introduced by Continuum Scattering Models on the Inferred Structural Properties of Proteins

Rohan S. Adhikari,[†] Dilipkumar N. Asthagiri,^{*,‡} and Walter G. Chapman^{*,†}

[†]*Department of Chemical and Biomolecular Engineering, Rice University, 6100 Main St.,
Houston, TX 77005, USA*

[‡]*Oak Ridge National Laboratory, One Bethel Valley Road, Oak Ridge, TN 37830-6012*

E-mail: asthagiridn@ornl.gov; wgchap@rice.edu

Contents

S.1 Workflow Depicting the Validation of Scattering Models	S2
S.1.1 Quantifying the Errors in R_g	S2
S.1.2 Quantifying the Over-Fitting from CRY SOL	S3
S.2 Simulation Details	S4
S.2.1 Simulations for Error Analysis using Contrast Matching	S4
S.2.2 Simulations for the χ^2 Fit Analysis using CRY SOL	S5
S.3 Contrast Estimation	S6
S.3.1 Determination of the Protein Surface	S6
S.3.2 Calculation of the Hydration Layer Contrast	S6
S.4 Scattering and R_g Computation	S8
S.4.1 Scattering Computations for Error Analysis using Contrast Matching	S8
S.4.2 Scattering Computations for the χ^2 Fit Analysis using CRY SOL	S9
S.4.3 Computation of R_g from Simulation Coordinates	S10
S.5 Validation of the Scattering Code	S13
S.6 The Effect of Thermal Fluctuations on R_g	S15
S.6.1 Details for the Thermally Fluctuating Protein Simulations	S15
S.6.2 Scattering Computation for Thermally Fluctuating Proteins	S15
S.6.3 Comparison of Scattering Methods	S16
References	S19

S.1 Workflow Depicting the Validation of Scattering Models

S.1.1 Quantifying the Errors in R_g

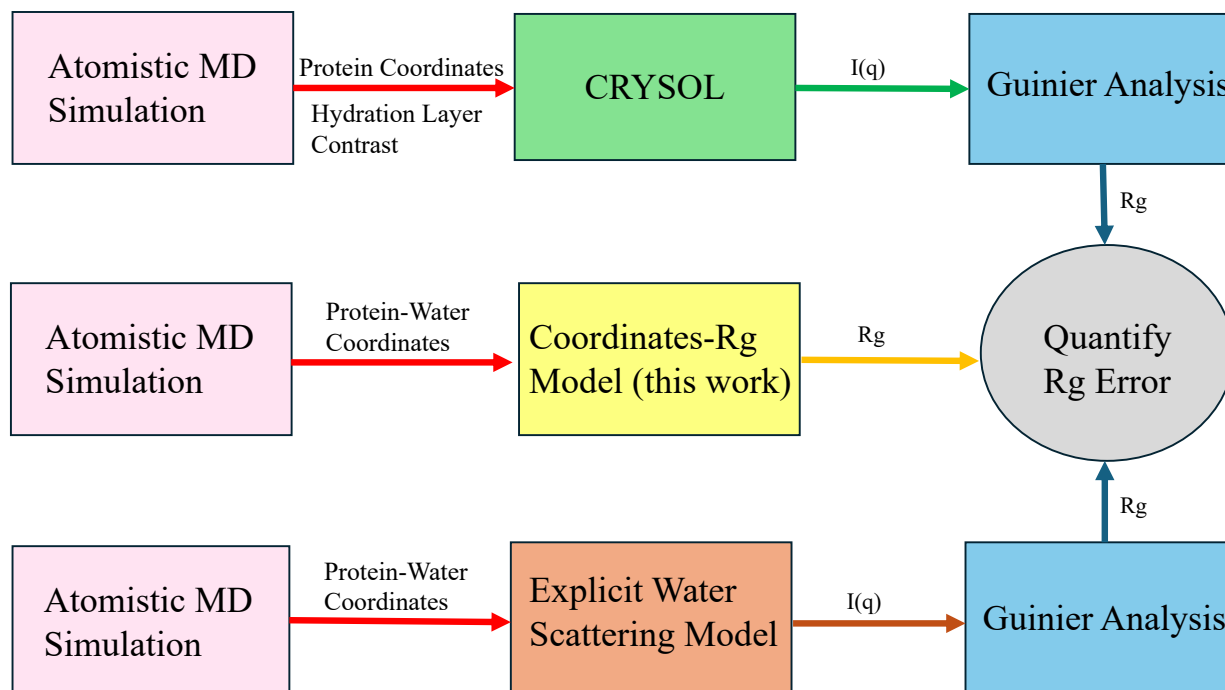


Figure S1: A flowchart depicting the philosophy of scattering model validation used in this work. An equation for calculating the radius of gyration (R_g) from the coordinates of an atomistic simulation is presented in this work. The R_g predicted by the CRY SOL model^{S1} and the explicit water scattering model^{S2} are compared to the coordinates-based model to quantify the errors in R_g .

S.1.2 Quantifying the Over-Fitting from CRY SOL

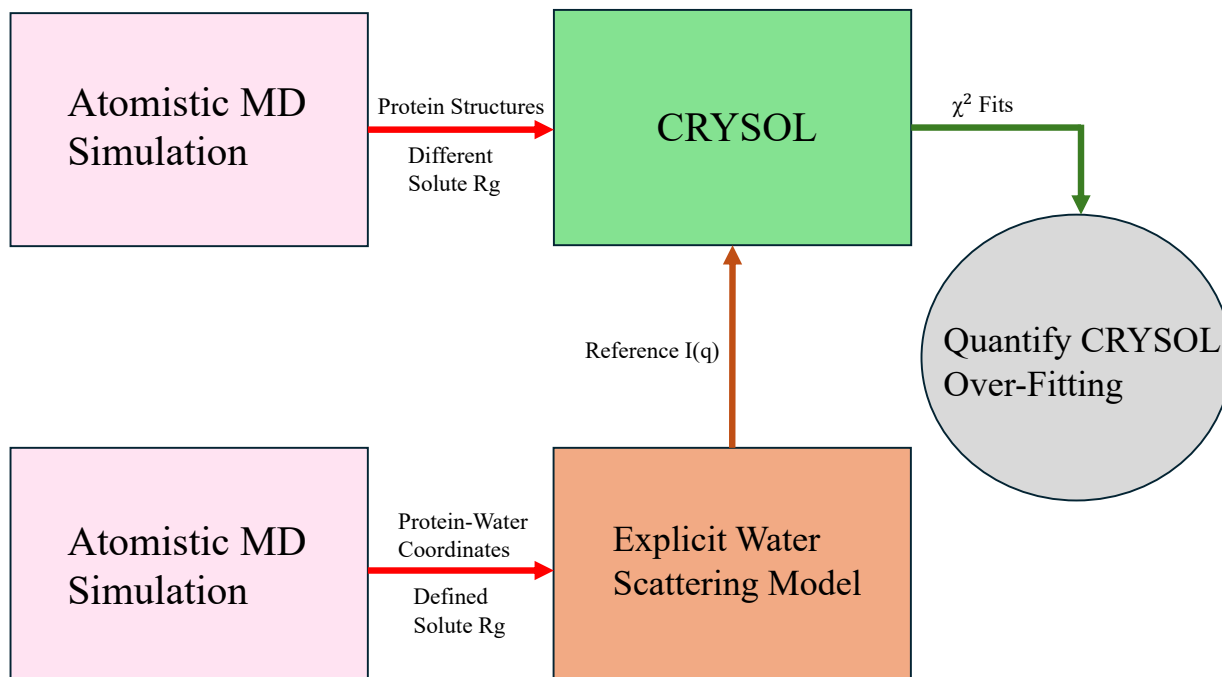


Figure S2: A flowchart depicting the quantification of over-fitting from the CRY SOL model.^{S1} The explicit water scattering model^{S2} with a frozen protein structure is used as a reference. Protein structures with varying solute R_g are fed into CRY SOL with the $I(q)$ from the explicit water scattering model. The χ^2 fits obtained from CRY SOL are studied as a function of the difference between the R_g of the solute structure in question and the R_g of the reference solute structure.

S.2 Simulation Details

S.2.1 Simulations for Error Analysis using Contrast Matching

For the analysis of errors from the CRY SOL model^{S1} and the Explicit Water Scattering Model (EWSM)^{S2} the MD simulations for 20 proteins were performed using the CHARMM36m (C36m)^{S3} force field for proteins and the modified TIP3P waters (mTIP3P).^{S4} All of the proteins were capped with ACE and NH2 terminal groups. An appropriate number of Na⁺ or Cl⁻ ions were added to counter balance the charges in the simulation system. The protein-water system containing the solute and 75000 mTIP3P waters were packed into a simulation box using PACKMOL.^{S5} The system was then energy minimized for 10000 steps to remove bad contacts. All simulations were carried out at 298.15 K and 1 atm pressure using a Langevin thermostat and a Langevin barostat on NAMD.^{S6} The simulations were run for 4 ns with a 2 fs time step by freezing the protein structure. (Note that one of us (DA) has shown that a 2 fs time-step with a rigid body description of water does violate equipartition between translational and rotational modes of water.^{S7} The effect is rather subtle, but one that is not expected to alter the main conclusions of this work, which was completed before the aforementioned work.)

After neglecting the first 2 ns of simulation, structures were saved every 2 ps to obtain a 1000 frames of simulated data. The Lennard-Jones (LJ) and electrostatic potentials were cut-off at 16 Å with a switching function for LJ interactions beginning at 15 Å. Neighbor lists of atom pairs were stored up to a distance of 18 Å. The long-range contribution to electrostatics was incorporated using the Particle Mesh Ewald (PME) approach, with a grid spacing of 1 Å.^{S8} The PDB codes for all 20 proteins and the errors from the scattering models are shown in Table S1. The 20 proteins used in our study were also used to predict the hydration layer around proteins in the HyPred program.^{S9}

Table S1: Details of the 20 proteins used in the analysis of the CRY SOL scattering model and the explicit water scattering model (EWSM). The errors from CRY SOL remain significant irrespective of the contrast in the hydration layer or the size of the system.

PDB Code	Number of Residues	Contrast [%]	ΔR_g (CRY SOL) [Å]	ΔR_g (EWSM) [Å]
1UBQ	76	19.77	2.06	0.02
6LYZ	129	19.08	2.44	0.01
1WLA	153	19.78	1.00	0.02
1CRC	105	21.00	2.40	0.01
1DF4	62	15.16	2.26	0.02
1DXG	36	19.07	0.98	0.03
1F94	63	17.57	2.30	0.01
1HYP	75	15.25	2.34	0.03
2L2P	56	16.63	1.70	0.02
1TIF	76	18.83	2.15	0.01
1UOY	64	19.14	2.43	0.02
1US0	314	23.73	1.70	0.01
1VCC	76	18.41	2.09	0.01
1YZM	46	16.45	1.68	0.03
2DOB	82	19.93	1.48	0.01
2PTN	230	19.79	1.82	0.02
2ZQE	80	19.35	2.36	0.01
3G19	84	18.52	1.80	0.01
3HGL	77	19.65	2.40	0.02
3LE4	55	15.10	2.55	0.02

S.2.2 Simulations for the χ^2 Fit Analysis using CRY SOL

For the computation of χ^2 as a function of ΔR_g (solute), 4 protein-water systems were simulated in the NVT ensemble. The simulations were carried out at high temperature (1000K) using a 1 fs time step for 2 ns. The average volume of the system from the previous simulation was used to define the simulation cell dimensions. Thermal fluctuations of the protein at high temperatures creates an R_g variation in the solute. 8 structures with R_g increasing in 0.5 Å intervals were selected from the structures obtained from each of the 4 simulations. The reference solute structure was chosen with an R_g 2.5 Å higher than the most compact selected structure and 1 Å lower than the most extended selected structure. The reference solute-water system was once again simulated by freezing the solute at 298.15 K and 1 atm (NPT ensemble) using the procedure described above. Cutoffs for the various

interactions were defined as described previously.

S.3 Contrast Estimation

S.3.1 Determination of the Protein Surface

The contrast in the 3 Å hydration shell around the solute is an important parameter that can be input into CRY SOL. To calculate the contrast in the system, the excluded volume of the solute first needs to be defined. We follow Virtanen et. al.^{S9} and define around 300 atom types to define a detailed surface for the protein. Each atom of each of the 20 amino acids constitutes a separate atom type. This is more detailed than previous studies where the protein is divided into 5 atom groups (C, N, O, S, H).^{S10} We simulated linear chains of each of the 20 amino acid residues in 34000 mTIP3P waters. The simulations were run at 298.15 K and 1 atm pressure for 4 ns with a 2 fs time step. Trajectories were stored every 2 ps in the last 2 ns after neglecting the first 2 ns. The closest distance of any water atom in the 1000 frames of simulated data to each of the atoms of the amino acid residues were recorded. This is treated as the surface radii of that particular atom type. The surface of the protein is then defined based on its amino acid sequence using the surface radii of the various atom types.

S.3.2 Calculation of the Hydration Layer Contrast

Once the protein surface was defined, the hydration layer was defined as the lowest volume that encapsulates all points that are less than 3 Å (> 0 Å) away from the protein surface. The contrast was then calculated using a reference bulk water simulation. The number of waters in the hydration shell surrounding the protein averaged over 1000 frames of the simulation ($\langle N_w^p \rangle$) and the number of waters in the same volume of the bulk water simulation ($\langle N_w^b \rangle$) were used to calculate the contrast in the hydration layer as shown in Eq. S.1

$$\delta\rho_h = \left(\frac{\langle N_w^p \rangle - \langle N_w^b \rangle}{\langle N_w^b \rangle} \right) \rho_b \quad (\text{S.1})$$

ρ_b is the electron density of the bulk solvent, which is $0.334 \text{ e}/\text{\AA}^3$ for water at 298.15 K and 1 atm pressure. For modified TIP3P waters the bulk electron density is slightly higher at $0.3389 \text{ e}/\text{\AA}^3$, which is the value we use in our calculations. The contrast calculated for each of the 20 proteins is shown in Table S1. The contrast so calculated ($\delta\rho_h$) and the bulk density of the buffer (ρ_b) were input into CRY SOL to analyze the errors from the model.

S.4 Scattering and R_g Computation

S.4.1 Scattering Computations for Error Analysis using Contrast Matching

The explicit water scattering model (EWSM)^{S2} is shown in Eq. S.2, where $A(\mathbf{q})$ is the amplitude from the protein-water simulation and $B(\mathbf{q})$ is the amplitude from the bulk water simulation.

$$\Delta I(q) = \left\langle \left| \langle A(\mathbf{q}) \rangle - \langle B(\mathbf{q}) \rangle \right|^2 + \left[\langle |A(\mathbf{q})|^2 \rangle - \langle |A(\mathbf{q}) \rangle|^2 \right] - \left[\langle |B(\mathbf{q})|^2 \rangle - \langle |B(\mathbf{q}) \rangle|^2 \right] \right\rangle_{\Omega} \quad (\text{S.2})$$

For the calculation of ΔR_g^{EWSM} by contrast matching, the equations to calculate $A(\mathbf{q})$ and $B(\mathbf{q})$ ^{S11} are shown in Eq. S.3.

$$\begin{aligned} A(\mathbf{q}) &= \sum_{j=1}^{N_A} n_e^A e^{-i\mathbf{q}\cdot\mathbf{r}_j}, \\ B(\mathbf{q}) &= \sum_{j=1}^{N_B} n_e^B e^{-i\mathbf{q}\cdot\mathbf{r}_j}, \end{aligned} \quad (\text{S.3})$$

Here the Fourier transform of the atomic coordinates are weighted by the electron numbers n_e^A and n_e^B to maintain consistency with the R_g calculation from coordinates. The background subtracted intensities from SAXS measurements are orientationally averaged due to the presence of a very high number of solutes which sample all orientations in solution.^{S12} The intensities calculated from simulation data also need to be orientationally averaged to match the experimental procedure. We perform an orientational average using the method of spirals^{S13} and 1500 direction vectors. Using 1500 direction vectors was found to be sufficient to obtain averages within 1 % error.^{S2} The waters in both the protein-water and bulk water simulations were chosen if they were within 3 Å of the protein surface to maintain consistency with CRY SOL.^{S14}

The R_g from the scattering curve was obtained using Guinier analysis.^{S15} In our calculation, we used 10 data points in the q range of $[0.001, 0.01] \text{ \AA}^{-1}$ to obtain R_g from the slope of the intensities as shown in Eq. S.4.

$$\ln \left[\frac{I(q)}{I(0)} \right] \approx -\frac{q^2 R_g^2}{3} \quad (\text{S.4})$$

S.4.2 Scattering Computations for the χ^2 Fit Analysis using CRY SOL

For the calculation of χ^2 fits from CRY SOL, EW SM is used as the reference. In this case the role of EW SM is to mimic experimental data. Hence we select all waters that are less than 7 \AA away from any solute atom in accordance with Ref. S2. The amplitude from the protein-water and bulk water simulations are now calculated using Eq. S.5 which incorporates the electron density clouds (form factors) of atoms ($f_j(q)$).

$$\begin{aligned} A(\mathbf{q}) &= \sum_{j=1}^{N_A} f_j(q) e^{-i\mathbf{q}\cdot\mathbf{r}_j}, \\ B(\mathbf{q}) &= \sum_{j=1}^{N_B} f_j(q) e^{-i\mathbf{q}\cdot\mathbf{r}_j} \end{aligned} \quad (\text{S.5})$$

To account for the polarizability of water, Sorenson et. al.^{S16} proposed a correction to $f_j(q)$ for water oxygens and hydrogens which is implemented in our work. The amplitudes A and B so calculated were then input into Eq. S.2 to calculate the background subtracted intensities. The background subtracted intensities were calculated for 101 q values in the range of $[0.0, 0.5] \text{ \AA}^{-1}$. The orientational averages were once again computed from the spiral method using 1500 direction vectors. We followed Park et. al.^{S2} and divided the 100 simulation frames into groups of 10 to obtain the error bars from block averaging.

S.4.3 Computation of R_g from Simulation Coordinates

In this work we have developed an equation for the radius of gyration from the coordinates of an explicit water simulation (R_g^{coor}). This is used as a benchmark to validate the R_g prediction from scattering models. In this section we show the steps involved in the development of Eq. 4 (main text). As we walk through the steps we appeal to the intuition of the reader. We begin with the equation for the radius of gyration for a system of N components from polymer theory (Eq. S.6).^{S17}

$$R_g^2 = \frac{\sum_{i=1}^N m_i |\mathbf{r}_i - \mathbf{r}_{\text{com}}|^2}{\sum_{i=1}^N m_i} \quad (\text{S.6})$$

Since we are comparing the R_g from coordinates to the predictions from a scattering model, we recognize that X-rays interact with the electrons of the system and not the nucleus. Hence we replace the masses of the atoms (m_i) in Eq. S.6 with their electron numbers (n_i^e). Which gets us to Eq. S.7.

$$R_g^2 = \frac{\sum_{i=1}^N n_i^e |\mathbf{r}_i - \mathbf{r}_{\text{com}}|^2}{\sum_{i=1}^N n_i^e} \quad (\text{S.7})$$

In background subtraction, the $I(q)$ of bulk waters is subtracted from the $I(q)$ of the protein-water solution. Hence we need to separate the number of atoms (N) in Eq. S.7 into the atoms in the protein solution (N_A) and atoms in the buffer solution (N_B). The atoms from the bulk water simulation (N_B) have negative weights to maintain consistency with the background subtraction procedure. With these modifications to Eq. S.7 we obtain Eq. S.8

$$R_g^2 = \frac{\sum_{N_A} n_A^e |\mathbf{r}_A - \mathbf{r}_{\text{com}}|^2 - \sum_{N_B} n_B^e |\mathbf{r}_B - \mathbf{r}_{\text{com}}|^2}{\sum_{N_A} n_A^e - \sum_{N_B} n_B^e} \quad (\text{S.8})$$

In SAXS measurements, the amplitudes from different conformations of proteins add up and the intensities captured by the receptor (square of the magnitudes of the amplitudes) are a reflection of the properties of the ensemble of structures. To mirror this, the information from the different frames of a simulation need to be superimposed so that the R_g obtained is a property of the simulation system as a whole. We take this fact into account by summing over the information from all frames of the simulation (N_F). Which leaves us with Eq. S.9. The number of atoms in the volume occupied by the protein and the hydration layer (N_A) and the number of bulk water atoms in the same volume (N_B) are functions of the simulation frame in consideration.

$$R_g^{\text{coor}} = \sqrt{\frac{\sum_{N_F} \sum_{N_A} n_A^e |\mathbf{r}_A - \mathbf{r}_{\text{com}}|^2 - \sum_{N_F} \sum_{N_B} n_B^e |\mathbf{r}_B - \mathbf{r}_{\text{com}}|^2}{\sum_{N_F} \sum_{N_A} n_A^e - \sum_{N_F} \sum_{N_B} n_B^e}} \quad (\text{S.9})$$

Similarly the equation for the center of mass transforms from Eq. S.10^{S17} to Eq. S.11.

$$\mathbf{r}_{\text{com}} = \frac{\sum_{i=1}^N m_i \mathbf{r}_i}{\sum_{i=1}^N m_i} \quad (\text{S.10})$$

$$\mathbf{r}_{\text{com}} = \frac{\sum_{N_F} \sum_{N_A} n_A^e \mathbf{r}_A - \sum_{N_F} \sum_{N_B} n_B^e \mathbf{r}_B}{\sum_{N_F} \sum_{N_A} n_A^e - \sum_{N_F} \sum_{N_B} n_B^e} \quad (\text{S.11})$$

Eq. S.9 is general and can be applied for any thickness of the hydration shell. Just as in the explicit water scattering model, the division of the protein-hydration layer complex into an excluded volume and hydration layer is also not necessary. The equation is also applicable for a control volume defined on the basis of the distance from the center of protein atoms instead of the protein surface. In this work to maintain consistency with CRY SOL, we define the hydration layer to be 3 Å away from the surface of the protein in all of our R_g^{coor} calculations. The R_g^{coor} calculation from Eq. S.9 and the calculation of intensities from the explicit water scattering model (Eq. S.2) were performed using in-house PYTHON scripts built atop the MDTraj library.^{S18}

S.5 Validation of the Scattering Code

To ensure that EWSM is being implemented correctly, we repeated the calculation in Ref. S2 for lysozyme (PDB code: 6LYZ). Lysozyme was modeled using the CHARMM22 (C22)^{S19} force field and simulated in 34000 TIP3P^{S20} waters on NAMD.^{S6} The solute was capped with N and C terminal groups using psfgen. The simulation was carried out at 277.15 K and 1 atm pressure using a 2 fs time step for 0.4 ns. Structures were saved every 2 ps after discarding the first 0.2 ns to obtain 100 frames of simulated data. The same procedure was used to simulate 34000 TIP3P waters and obtain 100 frames of data for the bulk solvent. Lennard-Jones (LJ) and electrostatic interactions were cut off at 16 Å. LJ was gradually turned off by switching the interactions at 15 Å. For long-range electrostatics we used PME with a grid spacing of 1 Å. Waters were chosen if they were less than 7 Å away from any solute atom. This envelope is large enough to account for all non bulk-like behavior of waters around the solute.^{S11}

The scattering model shown in Eq. S.2 was implemented using PYTHON scripts and the 100 frames were grouped into 10 blocks to estimate the error bars. The background subtracted intensities for lysozyme are shown in Fig. S3. The results are in excellent quantitative agreement with the predictions made by Park et. al.^{S2} The validated scattering code was then used to calculate the EWSM intensities for all the systems described in this study.

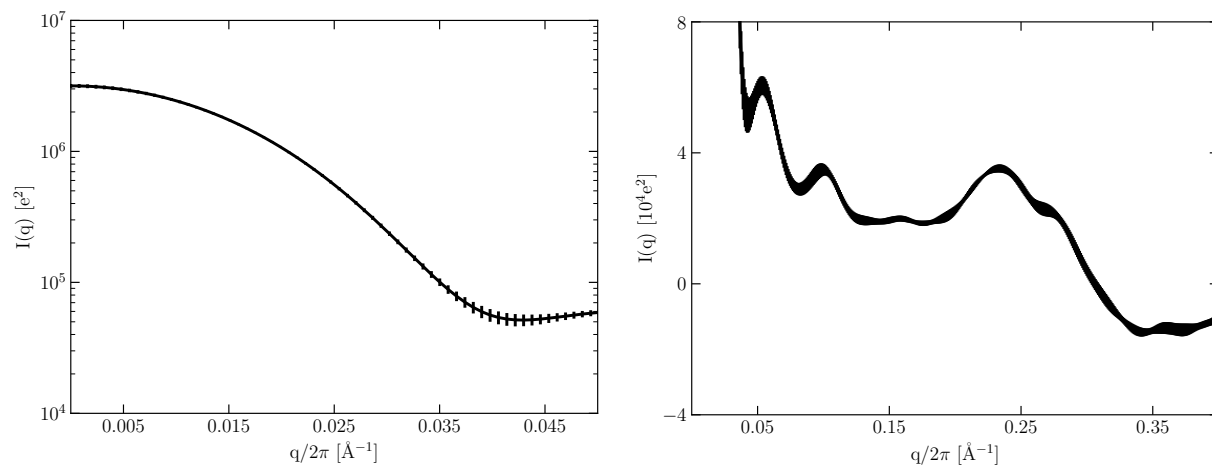


Figure S3: The background subtracted intensities for lysozyme are plotted against the magnitude of the momentum transfer vector ($\mathbf{q}/2\pi$). The intensities at low angle ($q/2\pi < 0.05 \text{ \AA}^{-1}$) are best represented on the log scale (left). The intensities at higher angles ($q/2\pi > 0.05 \text{ \AA}^{-1}$) have peaks and valleys that are best captured in the normal cartesian representation (right). The results are in excellent quantitative agreement with Park et. al.^{S2}

S.6 The Effect of Thermal Fluctuations on R_g

In this section we enquire if the thermal fluctuations of the solute causes a significant change in the R_g computed from Guinier analysis.

S.6.1 Details for the Thermally Fluctuating Protein Simulations

We took 4 proteins (PDB codes: 1DXG, 1F94, 1YZM, and 3LE4) and simulated them in explicit water by allowing for thermal fluctuations. The simulations were run at 298.15 K and 1 atm pressure for 30 ns. The first 10 ns were neglected and the trajectory file was updated every 2 ps. Out of the 10000 frames of simulated data, 1000 frames were chosen to emulate a Gaussian distribution in the R_g (solute) space. A protein structure with R_g at the center of the normal distribution (maximum probability) was chosen for the fixed solute scattering analysis. The simulation for the fixed solute in explicit water was performed as described previously and 1000 frames of simulation data were obtained. Scattering computations on the system were performed as described before. Error bars were calculated by block averaging using 5 blocks.

S.6.2 Scattering Computation for Thermally Fluctuating Proteins

The equation to calculate the scattering curve of a thermally fluctuating protein in explicit water is the same as the one for a frozen solute (Eq. S.2). However, the volume of the chosen envelope (control volume) varies.^{S11,S21} To study fluctuating proteins, the volume of the envelope must be large enough to contain the density fluctuations in water (around the solute) for every configuration. Knight and Hub^{S21} define the volume as an icosphere with 5120 vertices. In this work we divided the volume in $\phi - \psi$ space by using 10370 direction vectors. The 10370 direction vectors were moved from the center of the simulation box until they were 7 Å away from all solute atoms in all simulation frames. A water molecule was either chosen or neglected for analysis based on the r , θ , ϕ coordinates of its atoms. If any

water atom was closer to the center of the box than the maximum radii in the quadrant $[r_1, \theta_1, \phi_1]$, $[r_2, \theta_1, \phi_2]$, $[r_3, \theta_2, \phi_1]$, and $[r_4, \theta_2, \phi_2]$ defined by the direction vectors, it was chosen for analysis. A similar procedure was used to carve out an envelope in the bulk water simulation. The definition of the envelope and the calculation of the scattering from the solute in every frame are the only two differences between the scattering computation for a fluctuating solute and a frozen solute.^{S22}

S.6.3 Comparison of Scattering Methods

The contrast in the 3 Å hydration shell is compared for the fluctuating and frozen solutes in Table S2. For the contrast calculation of a thermally fluctuating protein, the hydration layer is dynamic and needs to be redefined every frame. The rest of the analysis remains the same. The contrast for all of the 4 proteins from the two methods are sufficiently close. There are regions around the solute that are quite favorable to the solvent, as the solute tumbles through the solution, the solvent molecules remain bound to the protein and move along with the solute. This is the reason the contrast calculated from the two methods remains fairly similar.

Table S2: Comparison of the hydration layer contrast and the radius of gyration (R_g) from Guinier analysis for the frozen and fluctuating solute system. Both methods yield similar properties on the macroscale.

PDB Code	Contrast (frozen) [%]	Contrast (fluctuating) [%]	R_g (frozen) [Å]	R_g (fluctuating) [Å]
1DXG	17.48 ± 0.33	17.48	11.95 ± 0.14	12.16
1F94	16.80 ± 0.09	16.29	11.93 ± 0.20	11.48
1YZM	15.82 ± 0.24	15.87	12.16 ± 0.12	12.29
3LE4	15.15 ± 0.15	15.41	12.03 ± 0.29	11.48

Scattering curve from the two methods are compared in Fig. S4. The two curves frequently overlap in the Guinier region. The R_g from Guinier analysis is also reported in Table S2, and is sufficiently close. This is due to the fact that the relative distance between the solute atom and the solvent molecules is preserved on a macroscale even as the protein tumbles in solution, causing little to no effect on the system R_g .

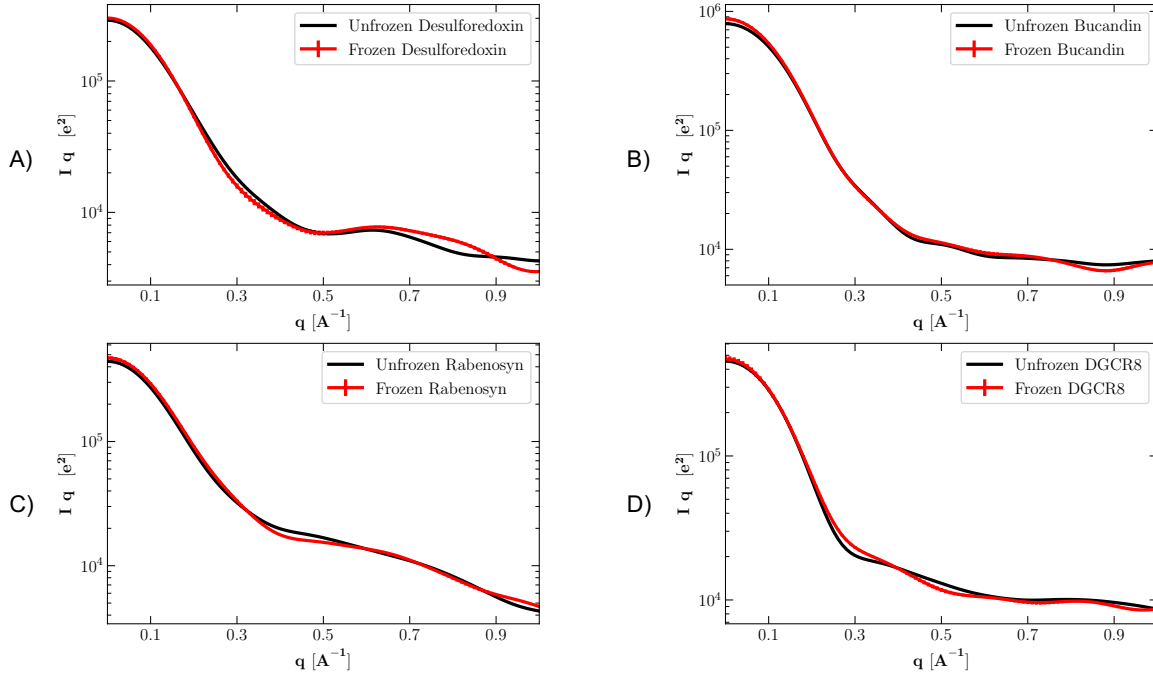


Figure S4: Comparison of the scattering curves from the two methods. Namely a frozen solute in explicit water (red) and a thermally fluctuating solute in explicit water (black). The error bars in the frozen solute scattering analysis are obtained by block averaging. The four proteins studied are desulforedoxin (1DXG) in (A), bucandin (1F94) in (B), rabenosyn (1YZM) in (C), and DGCR8 (3LE4) in (D).

The primary reason for the minor deviations in R_g and contrast is due to the comparison between two different ensembles. In our comparison of $R_g^{\text{CRY SOL}}$, R_g^{EWSM} , and R_g^{COOR} , all of the calculations pertained to the same ensemble, even though CRY SOL is a low information representation of the explicit solvent ensemble.^{S2} This allowed us to negate the variations that naturally arise during ensemble generation and isolate the errors from the scattering models. In our comparison of fluctuating and frozen proteins, the ensemble is necessarily different because they relate to different simulations. Hence it is not possible to isolate the differences in the scattering methods.

The average density of bulk waters over a 1000 frames is never identical between two independent simulations. There are always minor fluctuations in the average density. Chen et. al.^{S11} tracked these variations to tangible differences in intensities ($I(q)$) at low scattering angles. This probably explains the minor differences between the methods. Despite these complexities, the contrast and the R_g from the two methods are sufficiently close and we

conclude that the thermal fluctuations alone does not impact the R_g of the system.

References

- (S1) Svergun, D.; Barberato, C.; Koch, M. H. CRYSOLO—A Program to Evaluate X-Ray Solution Scattering of Biological Macromolecules from Atomic Coordinates. *J. Appl. Crystallogr.* **1995**, *28*, 768–773.
- (S2) Park, S.; Bardhan, J. P.; Roux, B.; Makowski, L. Simulated X-Ray Scattering of Protein Solutions using Explicit-Solvent Models. *J. Chem. Phys.* **2009**, *130*.
- (S3) Huang, J.; Rauscher, S.; Nawrocki, G.; Ran, T.; Feig, M.; De Groot, B. L.; Grubmüller, H.; MacKerell Jr, A. D. CHARMM36m: An Improved Force Field for Folded and Intrinsically Disordered Proteins. *Nat. Methods* **2017**, *14*, 71–73.
- (S4) Neria, E.; Fischer, S.; Karplus, M. Simulation of Activation Free Energies in Molecular Systems. *J. Chem. Phys.* **1996**, *105*, 1902–1921.
- (S5) Martínez, L.; Andrade, R.; Birgin, E. G.; Martínez, J. M. PACKMOL: A Package for Building Initial Configurations for Molecular Dynamics Simulations. *J. Comput. Chem.* **2009**, *30*, 2157–2164.
- (S6) Phillips, J. C.; Hardy, D. J.; Maia, J. D.; Stone, J. E.; Ribeiro, J. V.; Bernardi, R. C.; Buch, R.; Fiorin, G.; Hénin, J.; Jiang, W.; others Scalable Molecular Dynamics on CPU and GPU Architectures with NAMD. *J. Chem. Phys.* **2020**, *153*.
- (S7) Asthagiri, D. N.; Beck, T. L. MD Simulation of Water Using a Rigid Body Description Requires a Small Time Step to Ensure Equipartition. *J. Chem. Theory Comput.* **2024**, *20*, 368–374.
- (S8) Frenkel, D.; Smit, B. *Understanding Molecular Simulation: From Algorithms to Applications*; Elsevier, 2023.
- (S9) Virtanen, J. J.; Makowski, L.; Sosnick, T. R.; Freed, K. F. Modeling the Hydration

- Layer around Proteins: Applications to Small-and Wide-Angle X-Ray Scattering. *Biophys. J.* **2011**, *101*, 2061–2069.
- (S10) Virtanen, J. J.; Makowski, L.; Sosnick, T. R.; Freed, K. F. Modeling the Hydration Layer around Proteins: HyPred. *Biophys. J.* **2010**, *99*, 1611–1619.
- (S11) Chen, P.-c.; Hub, J. S. Validating Solution Ensembles from Molecular Dynamics Simulation by Wide-Angle X-Ray Scattering Data. *Biophys. J.* **2014**, *107*, 435–447.
- (S12) Svergun, D. I.; Koch, M. H.; Timmins, P. A.; May, R. P. *Small Angle X-Ray and Neutron Scattering from Solutions of Biological Macromolecules*; OUP Oxford, 2013; Vol. 19.
- (S13) Ponti, A. Simulation of Magnetic Resonance Static Powder Lineshapes: A Quantitative Assessment of Spherical Codes. *J. Magn. Reson.* **1999**, *138*, 288–297.
- (S14) Manalastas-Cantos, K.; Konarev, P. V.; Hajizadeh, N. R.; Kikhney, A. G.; Petoukhov, M. V.; Molodenskiy, D. S.; Panjkovich, A.; Mertens, H. D.; Gruzinov, A.; Borges, C.; others ATSAS 3.0: Expanded Functionality and new Tools for Small-Angle Scattering Data Analysis. *J. Appl. Crystallogr.* **2021**, *54*, 343–355.
- (S15) Cantor, C. R.; Schimmel, P. R. *Biophysical Chemistry: Part II: Techniques for the Study of Biological Structure and Function*; Macmillan, 1980.
- (S16) Sorenson, J. M.; Hura, G.; Glaeser, R. M.; Head-Gordon, T. What can X-Ray Scattering tell us about the Radial Distribution Functions of Water? *J. Chem. Phys.* **2000**, *113*, 9149–9161.
- (S17) Ivankov, D. N.; Bogatyreva, N. S.; Lobanov, M. Y.; Galzitskaya, O. V. Coupling between Properties of the Protein Shape and the Rate of Protein Folding. *PloS one* **2009**, *4*, e6476.

- (S18) McGibbon, R. T.; Beauchamp, K. A.; Harrigan, M. P.; Klein, C.; Swails, J. M.; Hernández, C. X.; Schwantes, C. R.; Wang, L.-P.; Lane, T. J.; Pande, V. S. MDTraj: A Modern Open Library for the Analysis of Molecular Dynamics Trajectories. *Biophys. J.* **2015**, *109*, 1528–1532.
- (S19) MacKerell Jr, A. D.; Bashford, D.; Bellott, M.; Dunbrack Jr, R. L.; Evanseck, J. D.; Field, M. J.; Fischer, S.; Gao, J.; Guo, H.; Ha, S.; others All-Atom Empirical Potential for Molecular Modeling and Dynamics Studies of Proteins. *J. Phys. Chem. B* **1998**, *102*, 3586–3616.
- (S20) Jorgensen, W. L.; Chandrasekhar, J.; Madura, J. D.; Impey, R. W.; Klein, M. L. Comparison of Simple Potential Functions for Simulating Liquid Water. *J. Chem. Phys.* **1983**, *79*, 926–935.
- (S21) Knight, C. J.; Hub, J. S. WAXSiS: A Web Server for the Calculation of SAXS/WAXS Curves based on Explicit-Solvent Molecular Dynamics. *Nucleic Acids Res.* **2015**, *43*, W225–W230.
- (S22) Hub, J. S. Interpreting Solution X-Ray Scattering Data using Molecular Simulations. *Curr. Opin. Struct. Biol.* **2018**, *49*, 18–26.